Journal of Alloys and Compounds 502 (2010) 127–131

Contents lists available at ScienceDirect

Journal of Alloys and Compounds

journal homepage: www.elsevier.com/locate/jallcom

Heteroepitaxial growth and surface electronic structures of ordered zinc oxide films on Mo(1 1 0) substrates

M.S. Xue, W. Li*, F.J. Wang, J.S. Lu, J.P. Yao

School of Materials Science and Engineering, Nanchang Hangkong University, Nanchang 330063, People's Republic of China

ARTICLE INFO

Article history:
Received 21 February 2010
Received in revised form 25 March 2010
Accepted 1 April 2010
Available online 22 April 2010

Keywords:
ZnO
Heteroepitaxial growth
Electronic structures

ABSTRACT

The preparation and surface electronic structures of ZnO thin films deposited on Mo(1 1 0) substrate by thermal evaporation under ultrahigh vacuum have been studied. Compared with insulating or semiconductive substrates, the metal substrate is of advantage to tune the surface electronic structures by electron spectroscopies owing to the elimination of surface charges. We found that 10^{-7} mbar or higher O_2 pressure was necessary for the formation of stoichiometric ZnO films, and the corresponding epitaxial relationship was identified as ZnO(0 0 0 1)/Mo(1 1 0). Furthermore, the surface electronic states of ZnO films originating from interband transition, surface and bulk plasma were analyzed. We revealed that for the polar ZnO(0 0 0 1) surface, O-terminated ZnO monolayer with rock-salt structure at the topmost surface was thermodynamically stable, implying a transition from the wurtzite to the rock-salt structure at the surface.

© 2010 Elsevier B.V. All rights reserved.

1. Introduction

Wide direct band gap semiconductors have received increasing attention due to their potential applications in solar cells, gas sensors, liquid-crystal displays, and especially in optoelectronic devices with short wave-length [1,2]. ZnO, as an oxide semiconductor with a band gap of 3.37 eV at room temperature (RT), is the most promising for the development of efficient ultraviolet devices [3]. In addition, the large exciton binding energy (60 meV at RT) of ZnO, compared with these of GaN (28 meV) and ZnSe (19 meV), is of advantage to stabilize excitonic emission processes and to solve the crucial issues such as large threshold current and short lifetime, which are the most important parameters for optoelectronic devices [4].

Over the past decade, the preparation of ZnO with various structures, e.g., thin films, nanoparticles, powders, nanowires and nanorods, which exhibit completely different physical and chemical properties, has attracted considerable attention because of their potential applications. Especially, to grow ZnO films with well desirable orientation, various preparation methods, including molecular beam epitaxy, chemical vapor deposition, pulsed-laser deposition, magnetron sputtering, thermal evaporation, etc, have been reported [1,2,5]. However, the quality of ZnO films has not been improved obviously, and some fundamental issues, such as microscopic formation mechanism and surface electronic structures, have remained unclear [1,6]. In order to reduce the lattice strain and dislocation density, a close lattice match between epitaxial ZnO films and substrates is favorable. Sapphire is commonly chosen as the substrates due to its low cost [2,3,7]. However, owing to a large lattice mismatch (18.4% with the 30° in-plane rotation) between ZnO (a = 3.250 Å, c = 5.213 Å) and sapphire (a = 4.754 Å, c = 12.99 Å), as-prepared ZnO films are characteristic of large mosaicity and defect-induced residual carrier concentrations [8]. To eliminate the in-plane domain rotation, to reduce the defects/vacancies, and to improve the stability of ZnO films, other substrates such as Si, SiC, GaAs, and $SrTiO_3$, have been utilized [1,9–11]. It is found that these substrates can improve the quality of ZnO films, but such semiconductive or insulating substrates can cause the so-called surface charge problem inducing by incident electrons of electronic spectroscopies (such as electron energy loss spectroscopy (EELS)), being of disadvantage to analyze their surface electronic structures. Contrarily, a conductive metal substrate is helpful for avoiding the surface charges.

Recently, single-crystal metals (especially refractory metals) as substrates have been widely used to prepare all kinds of ordered metal oxide films (such as MgO/Mo, Ti_xO_y/Mo, Fe_xO_y/Pt, Fe_xO_y/Ru) [12,13]. These thin oxide films on conductive metal substrates can offer a solution for the above-mentioned problem. Furthermore, from the view of fundamental research, to analyze the formation mechanism of ZnO films on a metal substrate is important in order to seek a better preparation method of ZnO films with high quality. It is therefore expected that the use of single-crystal metals as the substrates of ZnO growth cannot only improve the quality of films but also tune the surface structures.

* Corresponding author.
E-mail address: wenl@ualberta.ca (W. Li).

0925-8388/$ – see front matter © 2010 Elsevier B.V. All rights reserved.
doi:10.1016/j.jallcom.2010.04.115

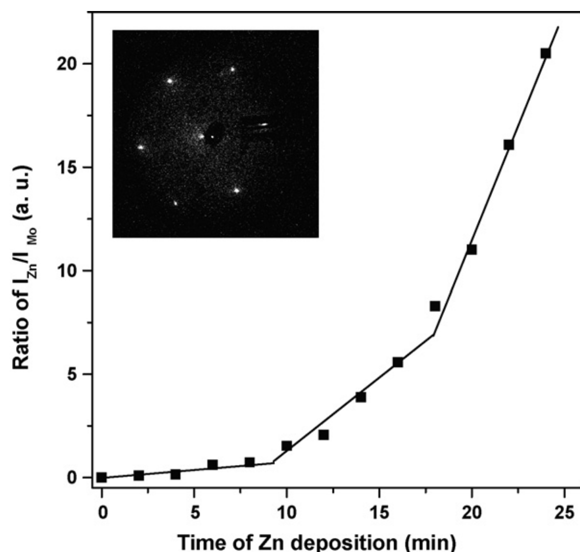

Fig. 1. AES intensity ratio of Zn LMM versus Mo MNN Auger lines as a function of Zn coverage at room temperature. The inset gives the LEED pattern of clean Mo(1 1 0) surface, E_p = 78 eV.

In the previous studies, several ordered oxide films (such as MgO(1 1 1) and FeO(1 1 1)) have been prepared on the metal Mo(1 1 0) substrate [14,15]. Since the structural symmetry of body-centric cubic Mo single-crystal along its (1 1 0) face is similar to that of wurtzite ZnO along the *c* plane, it is possible to prepare ordered ZnO films on Mo(1 1 0) substrate by the heteroepitaxial growth. In the present work, we try to realize this expectation and further investigate the electronic states and surface structures of the prepared ZnO films, which could provide useful information for the development of new optoelectronic devices.

2. Experimental detail

The preparations of ZnO films were performed in an ultrahigh vacuum (UHV) chamber with a base pressure of 1×10^{-10} mbar. The chamber is equipped with Auger electron spectroscopy (AES) with a cylindrical analyzer (CMA), low-energy electron diffraction (LEED), and EELS. A single-crystal Mo(1 1 0) substrate (with ±0.5° along the (1 1 0) direction), spot welded with Ta filament around its edge, was fixed to the sample pole. The sample temperature was monitored by a C-type thermocouple (W-5%Re/W-26%Re) that spot welded to the edge of the substrate.

Before growth, the substrate was cleared in $\sim 10^{-7}$ mbar oxygen ambience at ~1200 K using an electron beam heater, and followed by a subsequent flash to 1500 K without oxygen in order to remove surface contaminations (such as carbon and oxygen). The Zn source was made of a Zn wire (purity: 99.95%) entangled around a tungsten filament, which was resistively heated for the deposition of ZnO films on Mo(1 1 0). After the source was completely degassed by the thermal treatment, the evaporating rate of Zn was measured by monitoring the intensity ratio of Zn LMM to Mo MNN Auger lines via AES as a function of deposition time [16], as shown in Fig. 1. With the increase of Zn coverage, there were two obvious inflexions between linear regions, indicating a likely layer-by-layer growth of Zn on the Mo(1 1 0) substrate. Correspondingly, the measured deposition rate of Zn atoms was about 0.11 monolayer (ML) per minute. In the following work, the deposition rate of Zn was set to a constant value. A clear (1 × 1) LEED pattern was observed, as shown in the inset of Fig. 1, indicating the epitaxial growth of Zn films. The preparation of zinc oxide films was done by evaporating Zn in 10^{-8} to 10^{-6} mbar O_2 ambience at the substrate temperature of 300–450 K. The thickness of as-prepared ZnO films was about 5 nm.

The films were in situ monitored by AES, LEED and EELS. The EELS measurements were performed using an e-gun source with variable primary energies of 0–3000 eV. The direction of incident and reflected electron beam was normal to the sample surface. X-ray diffraction (XRD) was performed by means of a Siemens D500 diffractometer using the Cu Ka line at 1.5406 Å. The surface morphology was monitored by a XL30 S-FEG field emission scanning electron microscopy (SEM) with an accelerating voltage of 10 kV. All data were collected at RT.

3. Results and discussion

In order to investigate the formation of ZnO films, the preparation was conducted under different oxygen pressures, as shown in the AE spectra in Fig. 2a. For pure Zn films, there were no other elements detected, as indicated in curve a. In a lower O_2 pressure (10^{-8} mbar), the AE spectrum of as-prepared films shows the signal from Zn and O (curve b). Combined the intensity of O KLL and Zn LMM Auger lines with their corresponding atomic sensitive factors, the calculated ratio of Zn to O is about 1:0.5, i.e., part of Zn atoms are not oxidized [16]. When the O_2 pressure was enhanced to 10^{-7} mbar or higher (curve c), the ratio of Zn to O measured by AES was about 0.97:1, close to 1:1, indicating the formation of stoichiometric ZnO films in the range of the measured error.

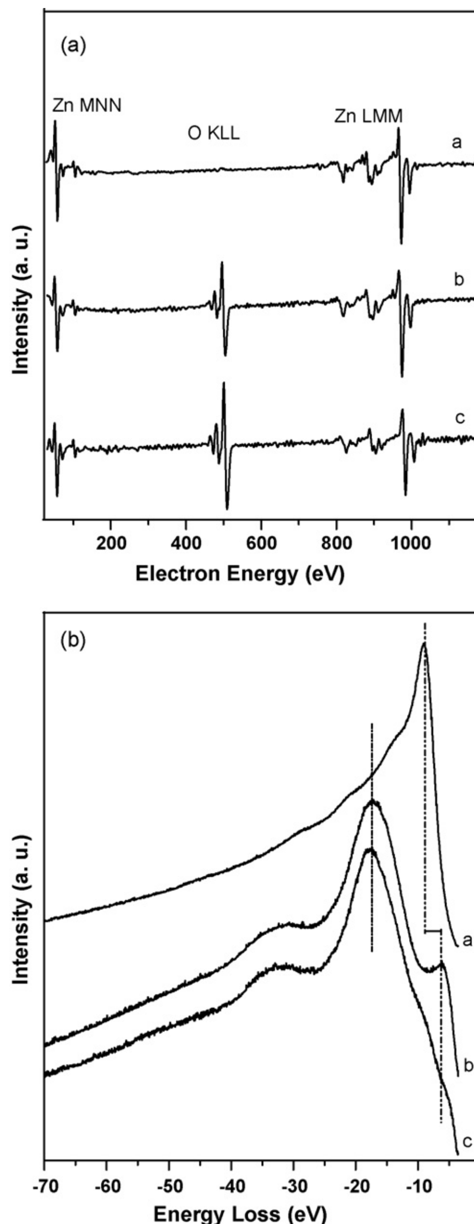

Fig. 2. (a) AE spectra of ZnO films prepared under different oxygen pressure: no oxygen exposure, 10^{-8} mbar and 10^{-7} mbar oxygen pressure (labeled as curve a–c), respectively and (b) corresponding EEL spectra of curve a–c in (a) with the primary incident energy of 300 eV.

Fig. 2b shows the EEL spectra of corresponding films at different O_2 pressures. For pure Zn films, there is only a strong peak at 5.0 eV (curve a), associated with the metallic Zn 2s state. For the films grown in 10^{-8} mbar O_2 ambience, a broad peak appears at 18 eV (curve b). Compared with pure Zn films, the peak at 5.0 eV slightly shifts to 4.7 eV due to the effect of oxidation states. However, the

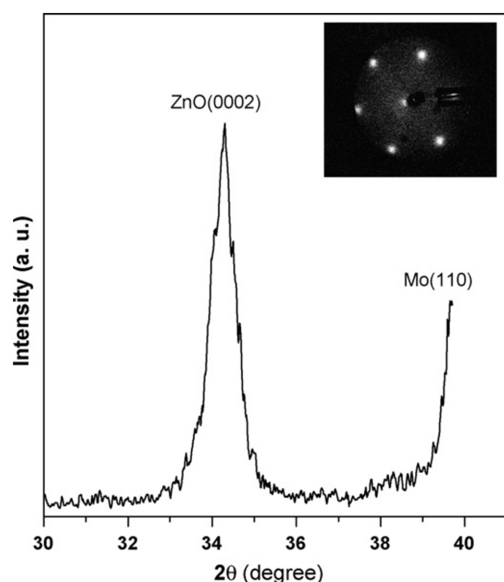

Fig. 3. X-ray diffraction pattern of ZnO films grown in 10^{-7} mbar oxygen pressure at RT. The inset shows the corresponding LEED pattern of curve c, E_p = 68 eV.

existence of this peak indicates that Zn films were not completely oxidized, in agreement with the result obtained from the AE spectrum. When the films were deposited in 10^{-7} mbar O_2 ambience, the peak characterizing metallic Zn disappeared and some new peaks became prominent (curve c). This indicated that these peaks associated with ZnO films.

During the growth process, the lattice epitaxy of the sample surface was in situ monitored by means of LEED. For 5 nm thick ZnO films prepared in 10^{-7} mbar O_2, a perfect hexagonal pattern was observed, as shown in the inset of Fig. 3, suggesting an ordered ZnO film. The typical XRD pattern from the same sample is shown in Fig. 3. One can see that besides the most intense peak around 40.5° resulting from the Mo(1 1 0) substrate [17], there is only one peak at 34.3°, corresponding to (0 0 0 2) direction of ZnO crystal [5,18]. Furthermore, the full width at the half maximum (FWHM) height of the diffraction peak is relatively broader than that of bulk ZnO crystal, being mainly relevant to the thickness of ZnO films [2,3,19]. For thin films, the effect of environmental noise on the measured signal and the interaction between films and substrates cannot been ignored. However, both the XRD and LEED results reveal the epitaxial growth of ZnO films on Mo(1 1 0) substrate, i.e., ZnO(0 0 0 1)/Mo(1 1 0).

It is worth to noting that there is a lattice strain between ZnO(0 0 0 1) films and Mo(1 1 0) substrate. Structurally, the lattice constants of Mo substrate along (1 1 0) face are a_0 = 2.74 Å and b_0 = 3.17 Å with a quasi-hexagonal symmetry. As for ZnO(0 0 0 1) face, it is characteristic of hexagonal symmetry with $a_0 = b_0$ = 3.25 Å. The lattice mismatches between ZnO(0 0 0 1) and Mo(1 1 0) are 18.6% and 2.7% along a_0 and b_0 directions, respectively, corresponding to tensile stress. Experimentally, we observed a hexagonal LEED pattern (the inset in Fig. 3) for ZnO films grown on Mo(1 1 0) substrate. The result indicates that the epitaxy of ZnO films was strongly dependent on the Mo(1 1 0) substrate, but the lattice strain was self-adjusted by the Zn–O bond. The possible reason is in that the tensile strain along a_0 direction was slightly bigger than that along b_0 direction, inducing a structural transformation from a monoclinic symmetry of Mo(1 1 0) surface to a hexagonal symmetry of ZnO(0 0 0 1) surface. Generally, a lattice mismatch between films and substrates larger than 10% is of disadvantage for the epitaxial growth. However, the present results indicate that the same/similar lattice symmetry is more important than the lattice mismatch for the epitaxial growth of metal oxide films on metal

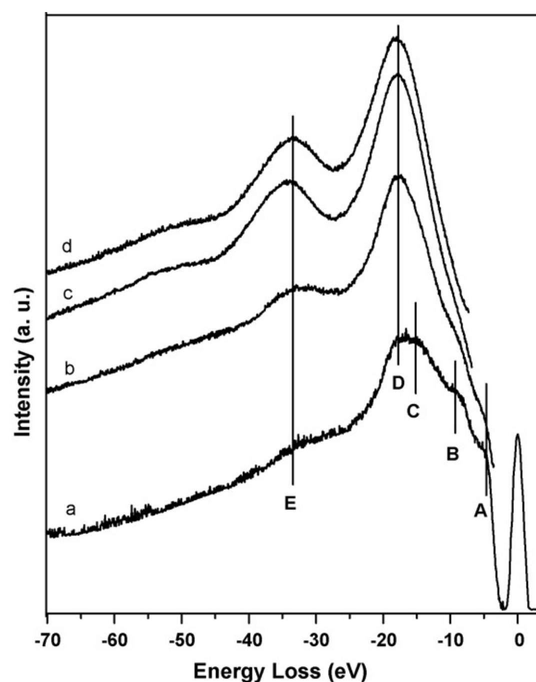

Fig. 4. EEL spectra of ZnO films with various primary incident energies: (a) 100 eV; (b) 300 eV; (c) 500 eV; and (d) 700 eV.

substrates. This is consistent with the previous studies. For example, the epitaxial growth of ZnO films on sapphire can be realized in spite of a lattice mismatch of 18.4% [1–4]. In addition, the similar phenomena were also found in the growth of other oxide films (such as MgO(1 1 1) and Fe_xO_y films) on Mo(1 1 0) regardless of the lattice mismatch [14,15].

The surface electronic structure of ZnO(0 0 0 1) films was also studied by EELS with the primary energies of 100, 300, 500 and 700 eV (Fig. 4). In EELS measurements, the electronic structure of the surface is exhibited by energy loss peaks originating from several inelastic interaction processes. In the low-energy loss region, bulk and surface plasma peaks are closely related to the dielectric response of the valence band, while in higher loss region, the near-edge fine structure is associated with the projected density of states in the conduction band [20]. In the practical experiments, most of loss peaks have mixed characters since the dipole transitions selection rules have been extended. If the initial state and the final state of a transition belong to different atom sites, the transition is detectable and is shown as main loss peaks near the valence band in the EEL spectra. From curve a in Fig. 4, one can see that the energy loss peaks locate at 4.7, 9.3, 15.2, 17.8 and 33.5 eV (labeled as A–E) below the Fermi level, respectively. With increasing the primary energy, the probing depth of the sample correspondingly increases. As a result, the peaks originating from bulk or surface structures can be distinguished. From E_p = 100–700 eV, the peaks A–E gradually become weak, while other peaks obviously become prominent. In particular, the peaks A and B originate from the interband transition, i.e., from O 2p to Zn 3 s in the valence region [21]. The two close peaks C and D are assigned to the surface and bulk plasma, respectively, whose intensity depends strongly on the primary energies. Peak E located at 33.5 eV is attributed to the interband transition, i.e., the transition from O 2s to Zn 3p [22]. These results are consistent well with the previous data from ZnO films [21–23].

Fig. 5 shows the surface morphology for ZnO films with a thickness of 5 nm deposited at 10^{-7} mbar O_2 at RT. It is seen that there are some nanometer-scale particles/clusters at the surface. Such particles/clusters observed by SEM are likely associated with the

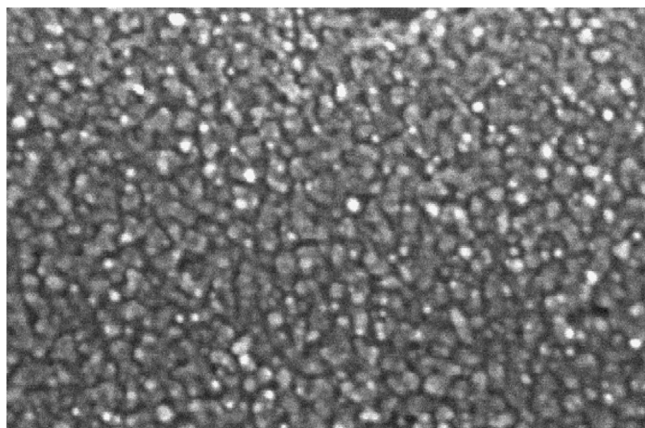

Fig. 5. SEM images (scan size: 400 nm × 600 nm) of 5 nm thick ZnO films.

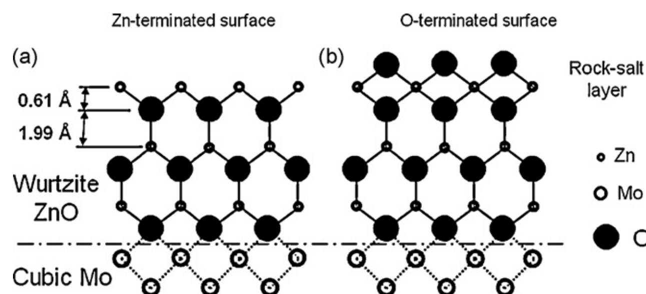

Fig. 6. Schematic of atomic arrangement of ZnO films on Mo(1 1 0) substrate: (a) Zn-terminated surface with wurtzite structure and (b) O-terminated surface with a possible rock-salt layer at the top surface.

surface polar instability of ZnO(0 0 0 1) films. In fact, the particles consisted of facets were also observed at the polar surfaces, e.g., at MgO(1 1 1) surfaces [24]. Polarity is a general phenomenon for the surfaces of ionic crystals along a certain direction exhibiting an alternative stacking of oppositely charged ionic planes parallel to the surface [25]. If the elastic deformation energy is largely suppressed, the polar films could self-assemble into different surface morphologies because of the minimization of electronic energy from the ionic charges on the polar surfaces [26]. In addition, it is noted that interfacial interaction, reconstruction, defects, stoichiometry as well as the growth techniques and methods can affect the surface morphology of the samples, which makes it difficult to determines surface fine structures of films.

The (0 0 0 1) face of ZnO films can be described as the stacking component of alternative planes composed of tetrahedrally coordinated O^{2-} and Zn^{2+} ions. The opposite charged ions bring positive Zn-(0 0 0 1) and negative O-(0 0 0 $\bar{1}$) polar surfaces, resulting in a normal dipole moment and spontaneous polarization along the *c*-axis. For ZnO, the macroscopic dipole moment can be canceled by many ways, such as charge transfer from O-terminated to Zn-terminated surface, hydrogen adsorption on the Zn- or O-terminated surfaces, rearrangement of surface atoms, and so on [1,25]. In the previous studies [27,28], based on atomic scale imaging the stabilization-induced faceting and triangular reconstruction at the Zn–ZnO(0 0 0 1) surface were reported. Furthermore, it was demonstrated that for ZnO films, the termination surfaces, i.e., Zn-(0 0 0 1) or O-(0 0 0 $\bar{1}$) plane at the surface can occur [29]. However, LEED cannot distinguish the terminated surfaces since both Zn-(0 0 0 1) and O-(0 0 0 $\bar{1}$) polar surfaces exhibit (1 × 1) hexagonal periodicity. There are also no clear images with atomic resolutions obtained by surface sensitive scanning tunneling microscopy (STM), besides some wide steps or small particles observed [27,28]. The previous work further indicated that Zn-terminated surface was stable by the removal of part Zn atoms from Zn-terminated surface [30,31]. However, the terminated planes are also significantly dependent on the growth conditions. On a clean surface, the topmost layer consists of Zn or O atoms with dangling bonds, which are connected with the O or Zn atoms in the second layer (Fig. 6a). Under O-rich condition (e.g., during growth at O_2 ambient), the dosage of oxygen is hard controlled, and the Zn atoms at Zn-terminated surface are easily covered by 1 ML O atoms, even if under UHV. Therefore, we believe that the topmost surface of ZnO films is most likely O-terminated. However, as-formed O plane is structurally instable. As shown in Fig. 6a, for Zn-terminated surface the topmost Zn–O bond length is 0.61 Å. If another O layer is absorbed to the surface, the Zn–O bond length will be 1.99 Å according to the lattice periodicity, being instable due to the large bond length and the existence of dangling bonds. However, if the O atoms are located at the bridge sites of two Zn atoms (as shown in Fig. 6b), the bond length will be shortened to 0.61 Å from 1.99 Å, which is helpful to maintain the stability of surface layers. Structurally, this will lead to a transition at the surface, i.e., from the wurtize to the rock-salt structure, benefiting to the stabilization of O-terminated surface. In fact, the rock-salt structure of ZnO were found at the initial growth step of ZnO films on sapphire by inserting a MgO(1 1 1) buffer layer [1,3]. Therefore, it is possible for ZnO films to form a rock-salt layer at the surface to keep the thermodynamical equilibrium.

4. Conclusions

The heteroepitaxial growth and surface electronic structures of ordered ZnO films have been investigated. We find that the formation of stoichiometric ZnO films need an oxygen pressure of 10^{-7} mbar or higher. By means of XRD and LEED, the lattice orientation of ZnO films on Mo(1 1 0) was along (0 0 0 1) direction. The several characteristic loss peaks given by EEL spectra appeared at the valence region, which were associated with interband transition, surface or bulk plasma. Based on the existence of O atoms, we indicated that it was difficult to characterize a clean Zn-terminated surface. Furthermore, we suggested that a rock-salt surface with O termination was possible. Although the present results elucidated the stability of polar ZnO(0 0 0 1) surfaces, its detailed microscopic mechanism and experimental evidence is needed in a further study.

References

[1] U. Ozgur, Ya.I. Alivov, C. Liu, A. Teke, M.A. Reshchikov, S. Dogan, V. Avrutin, S.-J. Cho, H. Morkoc, J. Appl. Phys. 98 (2005) 041301.
[2] Y. Chen, H. Ko, S. Hong, T. Yao, Appl. Phys. Lett. 76 (2000) 559.
[3] Y. Chen, S. Hong, H. Ko, M. Nakajima, T. Yao, Y. Segawa, Appl. Phys. Lett. 76 (2000) 245.
[4] M. Kubo, Y. Oumi, H. Takaba, A. Chatterjee, A. Miyamoto, M. Kawasaki, M. Yoshimoto, H. Koinuma, Phys. Rev. B 61 (2000) 16187.
[5] A. Meaney, J.R. Duclere, E. Mcglynn, J.P. Mosnier, R. O'Haire, M.O. Henry, Superlattice Microstruct. 38 (2005) 256.
[6] Y.M. Yu, B.G. Liu, Phys. Rev. B 77 (2008) 195327.
[7] Y. Chen, H. Ko, S. Hong, T. Yao, Y. Segawa, J. Cryst. Growth 214/215 (2000) 87.
[8] Y. Chen, S. Hong, H. Ko, V. Kirshner, H. Wenisch, T. Yao, K. Inaba, Y. Segawa, Appl. Phys. Lett. 78 (2001) 3352.
[9] S.J. Chen, Y.C. Liu, J.G. Ma, Y.M. Lu, J.Y. Zhang, D.Z. Shen, X.W. Fan, J. Cryst. Growth 254 (2003) 86.
[10] W.C. Shih, M.S. Wu, J. Cryst. Growth 137 (1994) 319.
[11] M. Kubo, Y. Oumi, R. Miura, A. Stirling, A. Miyamoto, M. Kawasaki, M. Yoshimoto, H. Koinuma, J. Chem. Phys. 109 (1998) 9148.
[12] C.T. Campbell, Surf. Sci. Rep. 27 (1997) 1.
[13] W. Weiss, W. Ranke, Prog. Surf. Sci. 70 (2002) 1.
[14] S.K. Purnell, X. Xu, D.W. Goodman, B.C. Gates, Langmuir 10 (1994) 3057.
[15] M. Fonin, Y.S. Dedkov, U. Rudiger, G. Guntherodt, Surf. Sci. 536 (2003) 61.
[16] K.D. Childs, B.A. Carlson, L.A. Lavanier, J.F. Moulder, D.F. Paul, W.F. Stickle, D.G. Watson, Handbook of Auger Electron Spectroscopy, 3rd edition, Physical Electronics, Inc., Minnesota, 1995, p. 17.
[17] E.B. Svedberg, T.S. Jemander, N. Lin, R. Erlandsson, G. Hansson, J. Birch, J.-E. Sundgren, Surf. Sci. 443 (1999) 31.

[18] Y.F. Mei, R.K.Y. Fu, G.G. Siu, P.K. Chu, C.L. Yang, W.K. Ge, Z.K. Tang, W.Y. Cheung, S.P. Wong, Mater. Sci. Semicond. Process. 7 (2004) 459.
[19] F.K. Shan, G.X. Liu, W.J. Lee, B.C. Shin, J. Appl. Phys. 101 (2007) 053106.
[20] J.L. Guyaux, Ph. Lambin, P.A. Thiry, Prog. Surf. Sci. 74 (2003) 319.
[21] Z.H. Zhang, X.Y. Qi, J.K. Jian, X.F. Duan, Micron 37 (2006) 229.
[22] M. Bouslama, M. Ghamnia, C. Jardin, M. Bouderbala, B. Gruzza, Vacuum 47 (1996) 1353.
[23] Y. Ding, Z.L. Wang, J. Electron Microsc. 54 (2005) 287.
[24] M. Gajdardziska-Josifovska, R. Plass, M.A. Schofield, D.R. Giese, R. Sharma, J. Electron Microsc. 41 (2002) s13.
[25] C. Noguera, J. Phys.: Condens. Matter 12 (2000) R367.
[26] J. Goniakowski, F. Finocchi, C. Noguera, Rep. Prog. Phys. 71 (2008) 016501.
[27] F. Ostendorf, S. Torbrugge, M. Reichling, Phys. Rev. B 77 (2008) 041405.
[28] J. Zuniga-Perez, V. Munoz-Sanjose, E. Palacios-Lidon, J. Colchero, Phys. Rev. Lett. 95 (2005) 226105.
[29] M.H. Du, S.B. Zhang, J.E. Northrup, S. Erwin, Phys. Rev. B 78 (2008) 155424.
[30] O. Dulub, U. Diebold, G. Kresse, Phys. Rev. Lett. 90 (2002) 016102.
[31] Z.X. Mei, X.L. Du, Y. Wang, M.J. Ying, Z.Q. Zeng, H. Zheng, J.F. Jia, Q.K. Xue, Z. Zhang, Appl. Phys. Lett. 86 (2005) 112111.